

**TABLE 3.** MPTA at 8 Weeks After Surgery

Group 1	Group 2 (Bone Wax)	Group 3 (TEC)
37	56	56
41	58	59
45	65	61
47	69	65
65	73	80
—	—	88
47.0	64.2	68.2

MPTA indicates medial proximal tibial angle; TEC, tissue-engineered construct.

hydrochloride (30 mg/kg of body weight) and intravenous injection of propofol (80 mg/kg). The proximal part of the left tibia was exposed through an anteromedial incision. A window in the medial side of the growth plate was first made using a high-speed dental burr (diameter, 2 mm). The drill was then introduced and passed centrally into the epiphyseal growth plate region. Physeal defects of 3 mm diameter and 5 mm depth were created. The periosteum,

subcutaneous tissue, and skin were then closed in layers. Rabbits were allowed free, weight-bearing movement with no immobilization of the legs. Operated rabbits were randomly divided into 3 groups as follows:

Group 1: nothing embedded into the physeal defect (n = 5).

Group 2: bone wax embedded into the physeal defect (n = 5).

Group 3: TECs were implanted into the physeal defect (n = 7).

**Evaluation of TEC Effectiveness**

Rabbits in all groups were killed at 4 or 8 weeks postoperatively. For radiographic evaluation, radiographs of the right (unoperated) and the left (operated) tibias were taken, and the medial proximal tibial angle (MPTA) was measured (Fig. 1).

For histologic evaluation, sections through the proximal tibia were made and stained with hematoxylin and eosin or safranin O. Histologic findings were scored according to a histologic grading scale (Table 1), with

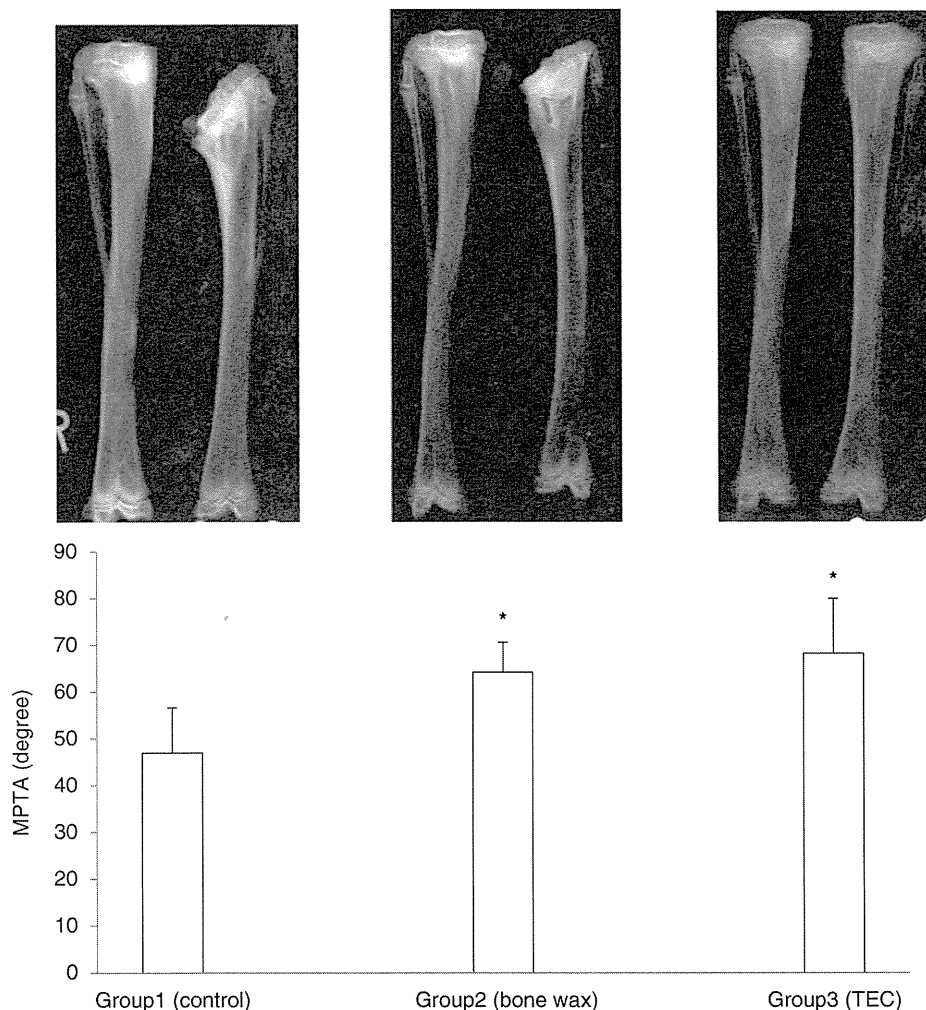


**FIGURE 3.** Medial proximal tibial angle (MPTA) at 8 weeks after surgery. Varus deformities were more severe in all groups than at 4 weeks. Varus deformities were significantly better in groups 2 (bone wax) and 3 (TEC) than in group 1. \*P<0.05.

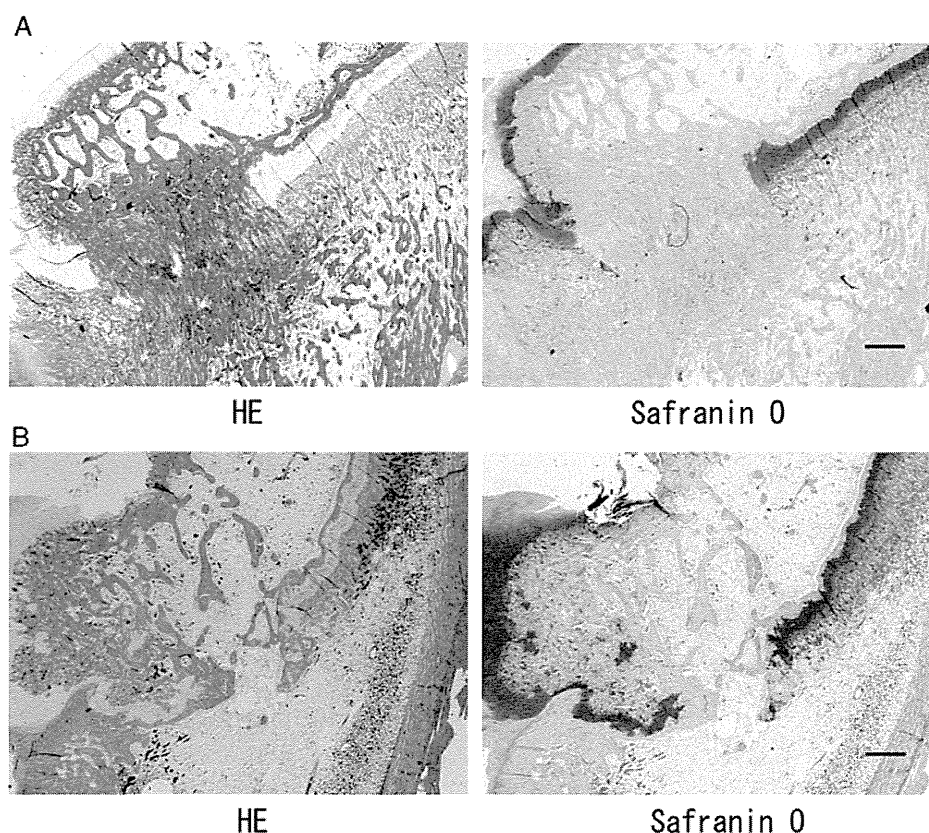


**FIGURE 4.** Histology in group 1. A, Histology at 4 weeks after surgery, showing bony bridge formation. B, Histology at 8 weeks. Bony bridge formation is increased and the epiphysis shows a wide connection with the metaphysis. Bar, 500  $\mu$ m. HE indicates hematoxylin and eosin.

higher scores indicating higher quality of the growth plate repair.

### Statistical Analysis

All data from at least duplicate samples are expressed as means  $\pm$  SD, and a minimum of 3 independent experiments were performed. Unpaired Student *t* test or analysis of variance for multiple comparisons were used for statistical analysis. Differences between experimental groups were considered significant for values of  $P < 0.05$ .

## RESULTS

### Radiographic Results

Group 1 demonstrated angular deformity of the left tibia, with a mean MPTA of 66.0 degrees (range, 62 to 75 degrees) at 4 weeks after surgery (Table 2 and Fig. 2) and 47.5 degrees (range, 37 to 65 degrees) at 8 weeks after surgery (Table 3 and Fig. 3). Radiography in this group showed partial growth arrest of the proximal medial tibias (Figs. 2, 3). The mean MPTA of the right tibia was 88.0 degrees.

The mean MPTA in group 2 was 79.8 degrees (range, 70 to 90 degrees) at 4 weeks after surgery (Table 2 and Fig. 2) and 64.2 degrees (range, 56 to 73 degrees) at 8 weeks after surgery (Table 3 and Fig. 3). Varus deformity

was milder than in group 1 at 4 weeks, postoperatively (Fig. 2). At 8 weeks after surgery, all cases showed varus deformity (Table 3 and Fig. 3). MPTA was significantly better than in group 1 at both 4 and 8 weeks after surgery (Figs. 2, 3).

The mean MPTA in group 3 was 80.9 degrees (range, 74 to 88 degrees) at 4 weeks after surgery (Table 2 and Fig. 2) and 68.2 degrees (range, 56 to 88 degrees) at 8 weeks after surgery (Table 3 and Fig. 3). Varus deformity was much milder than in group 1 at 4 weeks after surgery (Fig. 2), and MPTA in 3 of the 6 operated tibias was almost the same as in the unoperated tibias (Table 2). At 8 weeks postoperatively, 1 of the 6 operated tibias showed normal MPTA, and another case showed very little varus deformity. However, 4 of the 6 operated tibias showed varus deformity (Table 3 and Fig. 3). Compared with group 1, MPTA was significantly improved at both 4 and 8 weeks after surgery (Figs. 2, 3).

### Histologic Findings

In group 1, a bony bridge formation replaced the epiphyseal growth plate at the operated site, with the epiphysis showing a wide connection with the metaphysis at 4 weeks after surgery (Fig. 4A) and increased connection at 8 weeks (Fig. 4B).

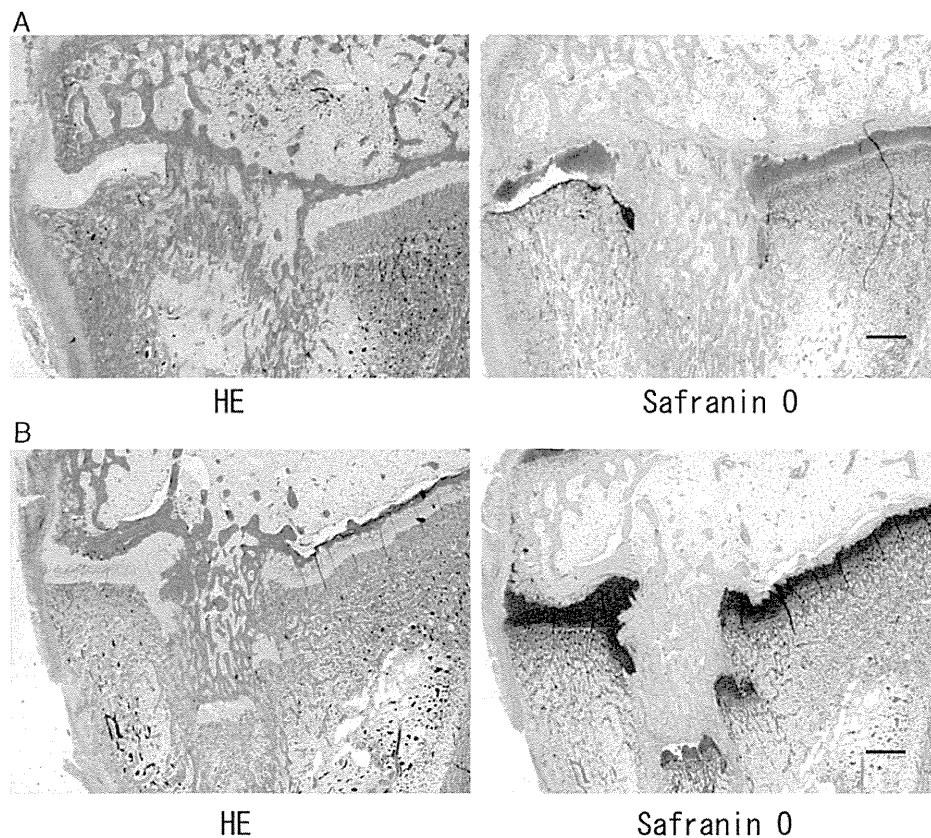


**FIGURE 5.** Histology in group 2 (bone wax). A, Histology at 4 weeks after surgery, showing partial bony bridge formation. B, Histology at 8 weeks, showing partial growth arrest over a wider area than at 4 weeks. Bar, 500 µm. HE indicates hematoxylin and eosin.

In group 2, all cases showed partial bony bridge formation. The transplanted bone wax remained at the operated site and showed no staining with hematoxylin and eosin or safranin O. However, some cases showed disappearance of transplanted bone wax and replacement with a bony bridge and growth plate-like tissue (Fig. 5). At 8 weeks after surgery, many cases showed a wider bony bridge area than at 4 weeks.

In group 3, all cases showed partial bony bridge formation. However, proliferative and prehypertrophic chondrocyte-like cells were seen at the operated site 4 weeks postoperatively (Fig. 6A). The cells took on a columnar arrangement like a normal physis and the physeal area was thickened (Fig. 6B). The cartilage matrix showed staining with safranin O, indicating the chondrogenic potential of MSCs in the TEC. Regeneration of the growth plate was recognized in the tibias without deformity (Fig. 6D).

### Histologic Scores

Histologic findings at 4 and 8 weeks after surgery were evaluated and rated using a histologic grading scale (Table 1). At 4 weeks after surgery, histologic scores for the repaired growth plate were higher in groups 2 and 3 than in group 1 (Table 4). At 8 weeks after surgery, histologic scores were lower in group 2 compared with scores

at 4 weeks (Table 5). Scores were significantly higher in group 3 than in group 2. At 8 weeks after surgery, group 2 showed a wider area of bony bridge formation, resulting in lower scores. Group 3 showed a thickened physeal area, resulting in higher scores.

### DISCUSSION

The physis has limited ability to repair itself. Injury and damage may thus lead to deformities and shortening of long bones by growth arrest with bone bridge formation. Various treatments such as gradual correction and bone bridge resection have been used with varying rates of success. In treatment by bone bridge resection, several types of interposition material have been used in clinical practice. Langenskiold<sup>21</sup> reported 38 cases of physeal bridge resection using autogenous body fat, suggesting that 82% of cases benefited from the procedure. Bright reported a series of 100 patients treated using silastic as the interposition material,<sup>22</sup> with 81% of patients demonstrating some growth after bridge resection, and 70% achieving good to excellent results. Klassen and Peterson<sup>23</sup> reviewed the Mayo Clinic experience with 50 cases of physeal bridge resection using cranioplast (methylmethacrylate) as the interposition material, reporting early closure of the operated physis. These findings

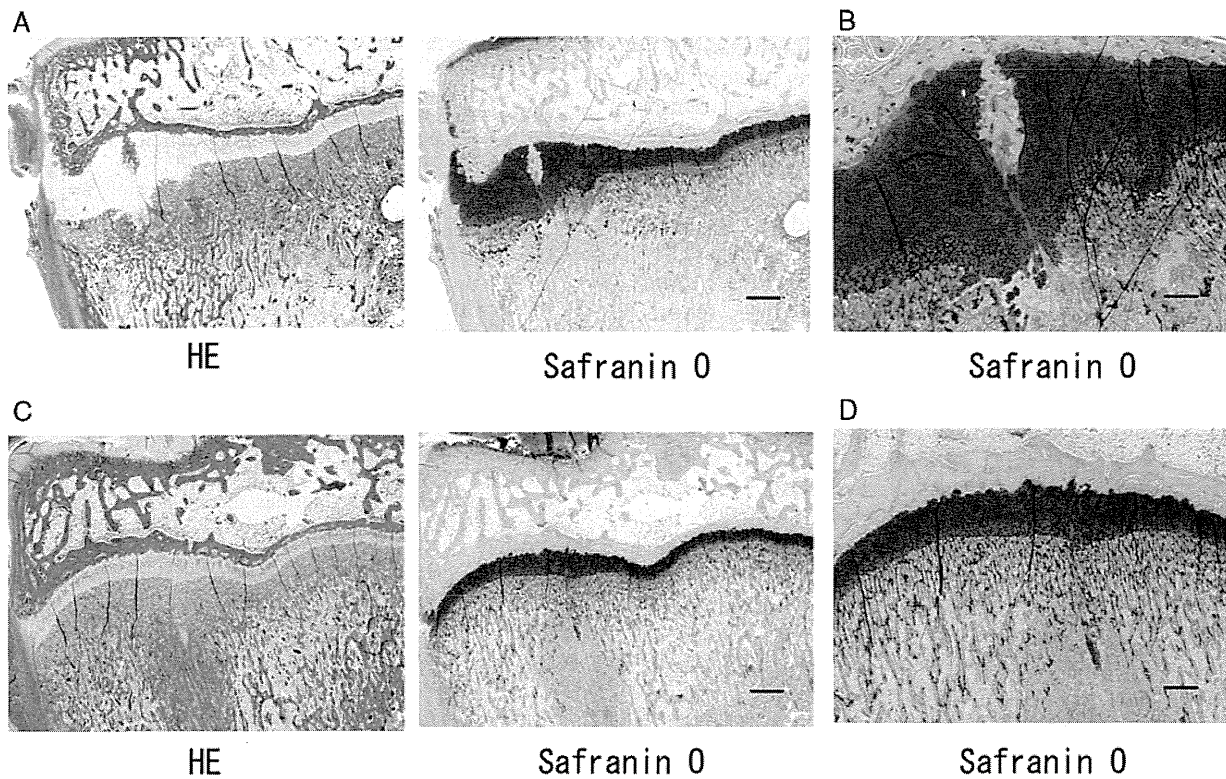


**FIGURE 6.** Histology in group 3 (TEC). A, Histology at 4 weeks after surgery, showing little bony bridge formation and repaired epiphyseal plate on the operated site. B, High-power section ( $\times 2$ ) of the new physal at 4 weeks after surgery. Proliferative and prehypertrophic chondrocyte-like cells are seen on the operated site, and the physal area is thickened. Bar, 500  $\mu$ m. C, Histology at 8 weeks after surgery, showing repaired epiphyseal plate. D, High-power section ( $\times 2$ ) at 8 weeks after surgery, showing the thickened physal area on the operated site. Bar, 500  $\mu$ m. HE indicates hematoxylin and eosin.

suggest that the interposition of fat, silastic, and other artificial materials might be associated with limitations to bone growth and several issues associated with long-term safety. We used bone wax as the interposition material in group 2. Many orthopaedic surgeons perform fat grafting in human epiphyseal plate injury. However, the bone wax is more difficult to be absorbed than the fat, and so, we used bone wax as the interposition material in this study.

The present study has demonstrated the feasibility of using a unique scaffold-free TEC from synovium-derived MSCs to repair the injured epiphyseal plate. The use of this unique TEC has the following benefits.

**TABLE 4.** Histologic Scores 4 Weeks After Surgery for the Repaired Growth Plate

Rabbit Number	Group 1	Group 2 (Bone Wax)	Group 3 (TEC)
1	0.0	1.0	3.0
2	0.5	2.5	3.0
3	0.5	3.0	3.5
4	4.0	6.0	3.5
5	5.5	8.5	5
6	—	—	6.5
7	—	—	7.0
Mean $\pm$ SD	2.1 $\pm$ 2.4	4.2 $\pm$ 3.0	4.5 $\pm$ 1.6

TEC indicates tissue-engineered construct.

First, TECs can be autogeneously developed without any need for an exogenous scaffold. Implantation of TECs thus has minimal risk of potential side effects induced by biological and artificial materials in the scaffold. Some papers have reported transfer of MSCs using scaffolds for the treatment of growth arrest.<sup>24,25</sup> No similar reports in the literature have mentioned the use of cultured MSCs without scaffolds to repair epiphyseal plate injury.

Second, TECs have the ability to allow chondrogenesis. We implanted pluripotent MSCs into the epiphyseal plate area, because reconstructing the columnar structure of the growth plate by MSCs in vitro is difficult.

**TABLE 5.** Histologic Scores 8 Weeks After Surgery for the Repaired Growth Plate

Rabbit Number	Group 1	Group 2 (Bone Wax)	Group 3 (TEC)
1	1.0	1.5	2.0
2	1.0	1.5	3.0
3	3.0	1.5	5
4	3.0	1.5	6.0
5	5.0	2.0	7.0
6	—	—	8.0
Mean $\pm$ SD	2.6 $\pm$ 1.6	1.6 $\pm$ 0.2	5.2 $\pm$ 2.5*

\*Significantly different from groups 1 and 2 ( $P < 0.05$ ). TEC indicates tissue-engineered construct.

The local *in vivo* environment might have stimulated differentiation of the TEC. For example, multiple cytokines such as parathyroid hormone-related protein and Indian hedgehog exist at various concentration gradients in the growth plate. We hypothesized that these cytokines could help with regeneration of the injured physis. Our results showed that using MSCs without scaffolds resulted in less bony bridge formation and contributed to longitudinal bone growth. In the control group, bony bridge trabeculae replaced the epiphyseal plate. In the TEC group, proliferative and prehypertrophic chondrocyte-like cells were seen on the operated site. These cells took on a slightly disordered columnar arrangement like a normal physis, and the physal area was thickened (Fig. 6). The implanted stem cells may thus show differentiation responses in the epiphyseal plate. In groups 2 and 3, the radiographic results were similar. However, the histologic scores of group 3 were significantly better than that of group 2. This is because the implanted stem cells could help the regeneration of the injured physis. We are planning to perform a longer duration of examination in the next study.

Further studies are needed to clarify the function of the new physis from the TEC with regard to bone growth and to examine applications in other large animals, including humans. This study used a small number of animals and only continued observations for 8 weeks. A larger number of subjects and a longer duration of examination are thus warranted. To attain more extensive chondrogenic differentiation responses, biological manipulation of the TEC may be required before implantation. This study used synovium-derived cells, which reportedly exhibit the most enhanced chondrogenic potential among mesenchymal tissue-derived cells.<sup>11</sup> If TECs are to be used for repair of epiphyseal injury in large animals such as humans, large quantities of cells will be needed. To overcome this problem, we are planning to use TECs cultured from induced pluripotent stem cells after confirming the quality of TECs developed using induced Pluripotent Stem cells in the next study.

### CONCLUSIONS

A scaffold-free 3D TEC made using cultured synovium-derived MSCs differentiated into proliferative and prehypertrophic chondrocyte-like cells. We have demonstrated the feasibility of a scaffold-free 3D TEC as a new approach for the repair of epiphyseal injury.

### REFERENCES

1. Langenskiold A. The possibilities of eliminating premature partial closure of an epiphyseal plate caused by trauma or disease. *Acta Orthopædica Scandinavica*. 1967;38:267-279.
2. Langenskiold A. An operation for partial closure of an epiphyseal plate in children, and its experimental basis. *J Bone Joint Surg Br*. 1975;57:325-330.

3. Broughton NS, Dickens DRV, Cole WG, et al. Epiphysiolysis for partial growth plate arrest. *J Bone Joint Surg Br*. 1989;71:13-16.
4. Langenskiold A. Surgical treatment of partial closure of the growth plate. *J Pediatr Orthop*. 1981;1:3-11.
5. Williamson RV, Staheli LT. Partial physal growth arrest: treatment by bridge resection and fat interposition. *J Pediatr Orthop*. 1990;10:769-776.
6. Bright RW. Operative correction of partial epiphysal plate closure by osseous-bridge resection and silicon-rubber implant. *J Bone Joint Surg Am*. 1974;56:655-664.
7. Macksoud WS, Bright R. Bar resection and silastic interposition in distal radial physal arrest. *Orthop Trans*. 1989;13:1-2.
8. Pittenger MF, Mackay AM, Beck SC, et al. Multilineage potential of adult human mesenchymal stem cells. *Science*. 1999;284:143-147.
9. Jankowski RJ, Deasy BM, Huard J. Muscle-derived stem cells. *Gene Ther*. 2002;9:642-647.
10. Bari CD, Dell'Accio F, Tylzanowski P, et al. Multipotent mesenchymal stem cells from adult human synovial membrane. *Arthritis Rheum*. 2005;44:1928-1942.
11. Sakaguchi Y, Sekiya I, Yagishita K, et al. Comparison of human stem cells derived from various mesenchymal tissues: superiority of synovium as a cell source. *Arthritis Rheum*. 2005;52:2521-2529.
12. O'Grady JE, Bordon DM. Global regulatory registration requirements for collagen-based combination products: points to consider. *Adv Drug Deliv Rev*. 2003;55:1699-1721.
13. Hunziker EB. Articular cartilage repair: basic science and clinical progress. A review of the current status and prospects. *Osteoarthritis Cartilage*. 2002;10:432-463.
14. Hunziker EB, Rosenberg LC. Repair of partial-thickness defects in articular cartilage: cell recruitment from the synovial membrane. *J Bone Joint Surg Am*. 1996;78:721-733.
15. Lee CR, Grodzinsky AJ, Hsu HP, et al. Effects of a cultured autologous chondrocyte-seeded type II collagen scaffold on the healing of a chondral defect in a canine model. *J Orthop Res*. 2003;21:272-281.
16. Drotka R, Bindreiter U, Macfelda K, et al. Marrow stimulation and chondrocyte transplantation using a collagen matrix for cartilage repair. *Osteoarthritis Cartilage*. 2005;11:877-886.
17. Nakamura N, Iwahashi T, Kawano K, et al. Healing of a chondral fragment of the knee in an adolescent after internal fixation. A case report. 2004. *J Bone Joint Surg Am*. 2004;86:2741-2746.
18. Ando W, Tateishi K, Hart DA, et al. Cartilage repair using an *in vitro* generated scaffold-free tissue engineered construct derived from porcine synovial mesenchymal stem cells. *Biomaterials*. 2007;28:5462-5470.
19. Ando W, Tateishi K, Katakai D, et al. *In vivo* generation of a scaffold-free tissue engineered construct (TEC) derived from human synovial mesenchymal stem cell: biological and mechanical properties, and future chondrogenic potential. *Tissue Eng Part A*. 2008;14:2041-2049.
20. Shimomura K, Ando W, Tateishi K, et al. The influence of skeletal maturity on allogenic synovial mesenchymal stem cell-based repair of cartilage in a large animal model. *Biomaterials*. 2010;31:8004-8011.
21. Langenskiold A. Surgical treatment of partial closure of the growth plate. *J Pediatr Orthop*. 1981;1:3-11.
22. Bright RW. Partial growth arrest: identification, classification, and results of treatment. *Orthop Trans*. 1982;6:65-66.
23. Klassen RA, Peterson HA. Excision of physal bars: the Mayo Clinic experience 1968-1978. *Orthop Trans*. 1982;6:65.
24. Li L, Hui JH, Goh JC, et al. Chitin as a scaffold for mesenchymal stem cells transfers in the treatment of partial growth arrest. *J Pediatr Orthop*. 2004;24:205-210.
25. Chen FC, Hui JHP, Chan WK, et al. Cultured mesenchymal stem cell transfers in the treatment of partial growth arrest. *J Pediatr Orthop*. 2003;23:425-429.



# Ovine synovial membrane-derived mesenchymal progenitor cells retain the phenotype of the original tissue that was exposed to in-vivo inflammation: evidence for a suppressed chondrogenic differentiation potential of the cells

Wataru Ando · Bryan J. Heard · May Chung · Norimasa Nakamura · Cyril B. Frank · David A. Hart

Received: 21 October 2011 / Revised: 12 January 2012 / Accepted: 8 February 2012 / Published online: 4 March 2012  
© Springer Basel AG 2012

## Abstract

**Background** The purpose of this study was to characterize the effect of post-surgery joint inflammation on the chondrogenic differentiation capacity of mesenchymal progenitor cells (MPCs) derived from the synovial membrane (SM).

**Methods** Six Suffolk-cross sheep were subjected to experimental anterior cruciate ligament (ACL) core surgeries. After they were killed 2 weeks after surgery, the volume of synovial fluid in the knees was measured and SM was collected for mRNA extraction and cell isolation. Cells were propagated and used for lineage-specific differentiation assays using cell pellet cultures and mRNA extraction. Chondrogenic differentiation assays in the presence of exogenous interleukin-1 $\beta$  (IL-1 $\beta$ ) were also performed.

**Results** The volume of synovial fluid from the operated knees was significantly greater than from the contralateral knees. Quantitative RT-PCR revealed that mRNA levels for IL-1 $\beta$  and matrix metalloproteinases-3 and -13 in SM from the operated knees were significantly higher than those from the contralateral knees. The size of MPC pellets from operated knees (opMPC) cultured in chondrogenic medium were significantly smaller than the corresponding pellets generated with MPCs from contralateral knees

(conMPC). Addition of 1–100 ng/ml IL-1 $\beta$  significantly suppressed the resultant size of chondrogenic cell pellets from normal ovine SM-MPC.

**Discussion** From these results, we conclude that cells from SM exposed to post-surgical inflammation are compromised by the inflammatory environment and that IL-1 $\beta$  can inhibit the latent chondrogenic potential of normal MPCs. This suggests that if MPCs from injured joints do contribute to cartilage repair, their endogenous repair potential may become compromised by such post-injury joint inflammation.

**Keywords** Chondrogenesis · Inflammation · Interleukin (IL) · Matrix metalloproteinases (MMP) · Mesenchymal progenitor cells (MPCs)

## Abbreviations

ACL	Anterior cruciate ligament
BM	Bone marrow
GAG	Glycosaminoglycan
IL-1 $\beta$	Interleukin-1 $\beta$
opMPC	MPC from operated knee
conMPC	MPC from contralateral knees
MPCs	Mesenchymal progenitor cells
MMPs	Metalloproteinases
OA	Osteoarthritis
SF	Synovial fluid
SM	Synovial membrane
TNF $\alpha$	Tumor necrosis factor- $\alpha$

Responsible Editor: John Di Battista.

W. Ando · B. J. Heard · M. Chung · C. B. Frank · D. A. Hart (✉)  
Faculty of Medicine, McCaig Institute for Bone and Joint Health, University of Calgary, 3330 Hospital drive, NW, Calgary, AB T2N4N1, Canada  
e-mail: hartd@ucalgary.ca

N. Nakamura  
Department of Orthopaedics, Osaka University Graduate School of Medicine, 2-2 Yamadaoka, Suita, Osaka 565-0871, Japan

## Introduction

Mesenchymal stem/progenitor cells (MSCs/MPCs) have the capacity to differentiate to a number of connective

tissue lineages such as osteogenic, chondrogenic, and adipogenic [1]. These cells may be isolated from various tissues such as bone marrow (BM), skeletal muscle, synovial membrane (SM), adipose tissue, umbilical cord blood, and placenta [1–6]. Among cells from a number of tissue sources, SM-MSCs/MPCs exhibit the most chondrogenic potential [7]. These cells are proposed to play an important role in the intraarticular environment to enhance endogenous repair and to be an appropriate cell source for cartilage regeneration therapy [8].

The surface ‘intima’ and the underlying ‘subintima’ are the two distinct anatomical layers forming the synovial tissue. The former layer is avascular and loosely organized, as it is not supported by a basement membrane, whereas the subintima consists of a network of connective tissue intermingled with cell types and blood vessels. The cell types predominantly present in this tissue are macrophage- and fibroblast-like synoviocytes [9] which are involved in the production of specialized matrix constituents such as hyaluronan, collagens, and fibronectin for the intimal interstitium and synovial fluid [10]. Although MSCs have been obtained from both synovium and synovial fluid, no specific location has been proposed where they may be present. In culture, cell surface markers, especially CD44<sup>+</sup>, are used to isolate these cells from a mixed population of cells of synovium or synovial fluid [11]. However, for the sheep model there is a shortage of reagents available.

Intraarticular injuries can lead to the onset and progression of osteoarthritis (OA). The mechanism of cartilage degradation is believed to be multi-factorial, and biological factors are believed to play important roles in the pathophysiology of OA [9, 12]. Such biological factors can aggravate cartilage degeneration by contributing to an unstable balance between catabolic and anabolic influences on cells. Inflammatory cytokines such as interleukin-1 $\beta$  (IL-1 $\beta$ ) and tumor necrosis factor- $\alpha$  (TNF $\alpha$ ) are known to be increased in the synovial fluid (SF) volume from patients with anterior cruciate ligament (ACL) injury [13–16], and these cytokines could potentially stimulate the synthesis of matrix degrading metalloproteinases (MMPs) [17, 18]. Such MMPs are believed to be partially responsible for the degradation of extracellular matrix in cartilage, contributing to the progression of OA.

The effect of intraarticular inflammation on the differentiation capacity of MSCs is controversial. It has been reported that advanced OA is correlated with reductions in the differentiation activity of human BM-MPCs [19], while normal cartilage contains CD105<sup>+</sup>/CD166<sup>+</sup> cells that have the phenotype of MPCs and the frequency of these cells has been reported to be increased in OA cartilage [20]. On the other hand, some studies have reported that BM-MSCs from patients with arthritis possess chondrogenic potential similar to BM-MSCs isolated from healthy donors [21].

Furthermore, the chondrogenic potential of human adult BM-MSCs has been reported to be independent of OA etiology [22]. The controversy is based, in part, on the fact that the differentiation capacities of BM-MPCs, and not SM-MPCs that have more chondrogenic potential than BM-cells [7], were compared in all of these previous studies.

Cells and tissues are exposed to the surgery-associated inflammation after surgery, and it is unclear how such inflammation affects both the endogenous tissues and cells in such environments in either the short term or long term. In spite of ACL reconstruction surgery, current ligament reconstruction procedures may not eliminate the progression of OA [23, 24], possibly related to inflammation in the joint. The purpose of this study was to characterize the effect of post-surgery inflammation on cells in the SM and the mesenchymal differentiation capacity of MPCs derived from SM exposed to short-term post-surgery inflammation in an established ovine model.

## Materials and methods

### Tissue collection, isolation and expansion of the cells

This study was performed in accordance with a protocol approved by the institutional animal ethics committee. Six skeletally mature 3–4-year-old female Suffolk-cross sheep were subjected to anatomically positioned reconstructive ACL autograft surgeries which were accomplished via an arthrotomy to the right stifle joint. The surgical procedure has been described in detail in Heard et al. [25]. Briefly, each surgical animal received an injection of Liqueamycin (Pfizer Canada, Inc., Kirkland, QC, Canada) 24 h pre- and post-surgery, Atro-Sa (Rafter Products, Calgary, AB, Canada), Acevet (Vetoquinol, Inc., Lavaltrie, QC, Canada), and Temgesic (Schering-Plough, Hertfordshire, UK) which were all administered as a pre-anesthetic cocktail. Under anesthesia, the patella was dislocated medially to expose the ACL. The proximal head of the lateral femoral condyle was the entry point for a guide pin that was inserted to mark the femoral insertion of the ACL. A dry pneumatic nitrogen drill with a hollow bore coring device was fitted over the guide pin and was used to core out the ACL from its femoral insertion and the ligament was later replaced at the same anatomical position. All animals were observed to be healthy and were killed 2 weeks after surgery.

The legs were severed from the hip joint within 30 min of death and incised for joint capsule exposure. Next, the synovial fluid was aspirated with a 10 ml syringe as much as possible, prior to collection of all other tissues of the joint capsule. Following collection, the total volume of the synovial fluid was measured. SMs were obtained

aseptically from both knees of each sheep. Half of each SM was used for cell isolation and the remainder was snap-frozen in liquid nitrogen and later used for mRNA extraction. The cell isolation protocol from SM was according to that described previously [8]. Briefly, the tissues were rinsed with phosphate-buffered saline (PBS; Invitrogen, Carlsbad, CA, USA), and then minced meticulously. The minced tissue was then digested with 0.2% collagenase (Worthington Biochemical Corp., Lakewood, NJ, USA) for 2 h at 37°C. After neutralization of the collagenase with basic culture medium containing high-glucose Dulbecco's modified Eagle's medium (DMEM) supplemented with 10% fetal bovine serum (FBS; Invitrogen, lot #439145) and 1% penicillin/streptomycin (Invitrogen), the cells were collected by centrifugation, resuspended in basic culture medium, and plated in T-25 cell culture flasks. For expansion, cells were cultured in the basic culture medium at 37°C in a humidified atmosphere of 5% CO<sub>2</sub>. The medium was replaced twice every week. After 7–10 days of primary culture, the cells were washed with PBS, harvested by brief treatment with 0.25% trypsin and 1 mM EDTA (Invitrogen), and replated in two T-75 flasks for the first subculture. Cells at passage 2 were used for the subsequent differentiation assays and mRNA analyses.

#### In-vitro chondrogenic differentiation assays

For cell pellet culture analysis,  $2 \times 10^5$  cells were transferred into 15 ml polypropylene tubes, centrifuged at 500g for 5 min to form a pelleted micromass at the bottom of the tube, and these pellets were then treated with chondrogenic medium for 14 days with medium changes twice weekly. The chondrogenic medium consisted of DMEM supplemented with 1% insulin–transferrin–selenium supplement (Invitrogen), 100 nM dexamethasone (Sigma-Aldrich), 0.2 mM ascorbic acid 2-phosphate (Asc-2p; Sigma-Aldrich) and 500 ng/ml recombinant human BMP2 (PeproTech Inc., Rocky Hill, NJ, USA) [26, 27]. After 14 days of culture, macroscopic analysis was performed by stereomicroscopic procedures [27]. The images were analyzed by Scion image (Scion Corporation, Frederick, MD, USA), and then the cross-sectional areas of the resultant cell pellets were calculated as a parameter of pellet size. Glycosaminoglycan (GAG) levels in the pellet cultures were measured as previously described [28]. Briefly, cell pellets were digested with a 0.25 mg/ml papain solution (Sigma), and then the eluates were assessed using the 1,9-dimethylmethylene blue binding assay. Absorbance of the extracted product was measured using a spectrophotometer (Benchmark Plus; Bio-Rad, Hercules, CA, USA) at 510 nm. The total amount of protein was also

measured by the bicinchoninic acid protein assay method (Sigma) for normalization. Each of the cell pellet samples was assessed in duplicate.

For mRNA extraction, cells were seeded in 12-well plates at a density of  $1 \times 10^4$  cells/cm<sup>2</sup> in the basic culture medium. The medium was then changed to the chondrogenic induction medium at 24 h and day 3. Samples were collected at day 7 and mRNA extracted using the TRIspin method [29].

#### In-vitro osteogenic differentiation assays

Cells were seeded in 24-well plates at a density of  $1 \times 10^4$  cells/cm<sup>2</sup> in the basic culture medium. After the medium was changed to an osteogenic medium at 24 h, cells were continuously cultured with medium changed twice weekly. Osteogenic medium consisted of basic culture medium, 100 nM dexamethasone, 10 mM  $\alpha$ -glycerophosphate, and 0.2 mM Asc-2P (all from Sigma-Aldrich) [3]. At day 10, some cells were fixed with 10% neutral buffered formalin and then stained with Alizarin Red S solution (Sigma-Aldrich) for 3 min to stain for calcium deposits. For measurement of calcium deposition, other cell preparations were lysed in 10% formic acid and calcium content in solutions was measured using a colorimetric kit (Arsenazo III; Diagnostic Chemicals Limited, Charlottetown, PE, Canada). Each of the samples was assessed in duplicate.

#### In-vitro adipogenic differentiation assays

Cells were seeded in 24-well plates at a density of  $1 \times 10^4$  cells/cm<sup>2</sup> in basic culture medium for 2 days. The medium was then shifted to adipogenic induction medium consisted of basic culture medium supplemented with 0.5 mM 3-isobutyl-1-methylxanthine, 1  $\mu$ M hydrocortisone, 0.1 mM indomethacin and 5 mM octanoate. After 2 days, the medium was replaced with basic culture medium supplemented with 5  $\mu$ g/ml insulin and 5 mM octanoate (all from Sigma-Aldrich) [1, 30]. Cells were cultured for an additional 6 days before staining with Oil Red O (Sigma-Aldrich). After fixation in 10% neutral buffered formalin, the cells were immersed in a 60% Oil Red O solution (Sigma) for 30 min. The cultures were then washed thoroughly with distilled water to remove background Oil Red O staining. The associated Oil Red O was eluted with 100  $\mu$ l of 100% isopropanol, and the optical density of 70  $\mu$ l of the eluates was quantified using a spectrophotometer at 510 nm [31]. The absorbance of the cells cultured in the basic culture medium was used as the background value to compare each sample. Each of the eluates was tested in duplicate.



### Chondrogenic differentiation assay in the presence of exogenous IL-1 $\beta$

To examine the effect of IL-1 $\beta$  on chondrogenesis of MPCs, normal SM were obtained from normal sheep not involved in the ACL core surgery aims of the study. Cells were isolated and expanded using the same procedure as described above. Pelleted micromasses from these cells were cultured in the chondrogenic medium containing human 0–100 nM IL-1 $\beta$  (PeproTech) starting on day 1. At day 14, the cross-sectional areas of the resultant cell pellets were calculated as described above.

### Semi-quantitative real-time polymerase chain reaction (RT-PCR) and real-time quantitative RT-PCR (RT-qPCR) analysis

Total RNA was isolated from both SM tissue and the cells isolated from these tissues using the TRIspin method [29]. One microgram of total RNA from each sample was initially reverse-transcribed with random RT primers using an Omniscript RT kit (Qiagen, Hilden, Germany). Type II collagen expression was assessed for determining the extent of chondrogenesis by semi-quantitative RT-PCR using specific PCR primers as described in Table 1. All amplicons were sequenced to confirm specificity for sheep molecules (data not shown). The protocol described previously was used throughout [32]. The optional cycle number for both col2a1 and 18S was 24. Amplicons were separated on a 2% agarose gel

followed by staining with ethidium bromide and band detection using a GelDoc system (Bio-Rad). RT-qPCR was performed using Bio-Rad iQ SYBR Green Supermix (Bio-Rad) as previously described [33]. PCR primers and the annealing temperatures are listed in Table 1. Amplification and detection were performed using an iCycler Thermal Cycler (Bio-Rad). To normalize for input load of cDNA between the samples, 18S was used as an endogenous standard for normalization. Preliminary studies indicated that 18S mRNA levels did not change during the response to injury (data not shown). The quantification of the relative fold change between samples was analyzed using iCycler iQ Optical System Software, ver. 3.0a (Bio-Rad). Each of the cDNA preparations was tested in duplicate. The standard curve method was used to quantify the relative fold change between samples. The correlation coefficient of each standard curve was  $\sim 0.99$  [34].

### Statistical analysis

The results are presented as mean  $\pm$  SD. Measurement of synovial fluid volume, mRNA levels, and adipogenesis parameters were analyzed by the Mann–Whitney  $U$  test. Measurements of chondrogenesis and osteogenesis parameters were analyzed by ANOVA with Bonferroni's multiple comparison  $t$  test. STATVIEW version 5.5 software performed statistical calculations (SAS Institute, Cary, NC, USA) and significance was set at  $p < 0.05$ .

**Table 1** Primer sequences and conditions for PCR analysis of sheep mRNA

Gene	Gene ID	Primer sequence	$T_m$ ( $^{\circ}$ C)	Size (bp)
18S (human)	X03205	F: TGGTCGCTCGCTCCTCTCC R: CGCCTGCTGCCTTCCTTGG	65	360
Col2a1 (bovine)	X02420	F: GAGCAGCAAGAGCAAGGACAAG R: GTAGGTGATGTTCTGAGAGCCCTC	53	163
IL-1 $\beta$	NM_001009465	F: CGAACATGTCTTCCGTGATG R: TCTCTGTCCTGGAGTTTGCAT	57	144
IL-6	NM_001009392	F: ACAGCAAGGAGACTGGCA R: GCCGAGCTACTTCATCCGA	57	396
MMP-2	AF267159	F: CTACCACCTCCAACACTACGAT R: AGAATGTGGCTACTAGCAG	57	412
MMP-3 (bovine)	AF135232	F: TTAGAGAACATGGGGACTTTTTG R: CGGGTTCGGGAGGCACAG	65	360
MMP-13	AY091604	F: GGTCTGTTGGCTCACGCTTTCC R: GAGTGCTCCTGGGTCCTTGG	65	171

*18S* 18S ribosomal RNA gene, *Col2a1* collagen type 2a1, *IL-1 $\beta$*  interleukin-1 $\beta$ , *IL-6* interleukin-6, *MMP2* matrix metalloproteinase-2, *MMP3* matrix metalloproteinase-3, *MMP13* matrix metalloproteinase-13

**Results**

Synovial fluid volumes are increased and mRNA levels for IL-1 $\beta$  and matrix metalloproteinase (MMP)-3 and -13 are upregulated in SM after surgery

At 2 weeks after surgery, the knees were swollen with significantly increased SF volumes in operated knees ( $9.21 \pm 4.00$  ml) compared to the contralateral knees ( $0.583 \pm 0.342$  ml,  $p = 0.003$ ). Thus, this time point was chosen to assess the acute response to injury/surgery. To further investigate the differences in SM between operated knees and contralateral knees, mRNA levels for catabolic biomarkers were assessed. RT-qPCR revealed that mRNA levels for IL-1 $\beta$ , MMP-3, and MMP-13 normalized to 18S in SM from the operated knees were significantly higher than those from contralateral knees (Fig. 1a–c). Regarding

mRNA levels for IL-6 and MMP-2, significant differences were not uniformly detected (Fig. 1d, e). These results suggested that surgical invasion of the joint leads to induction of selective inflammatory mediators in the joint, and this is reflected in elevated mRNA levels for a subset of catabolic biomarkers in the SM tissue.

Cells from SM exposed to post-surgery inflammation exhibit diminished chondrogenic potential compared to those from non-operated contralateral knees

Cells were isolated from the operated (opMPC) and contralateral (conMPC) knees. To evaluate the chondrogenic potential of both opMPCs and conMPCs, cell pellets were cultured in chondrogenic medium. Pellets from cells cultured in chondrogenic medium were significantly larger than those for the corresponding cells cultured in control

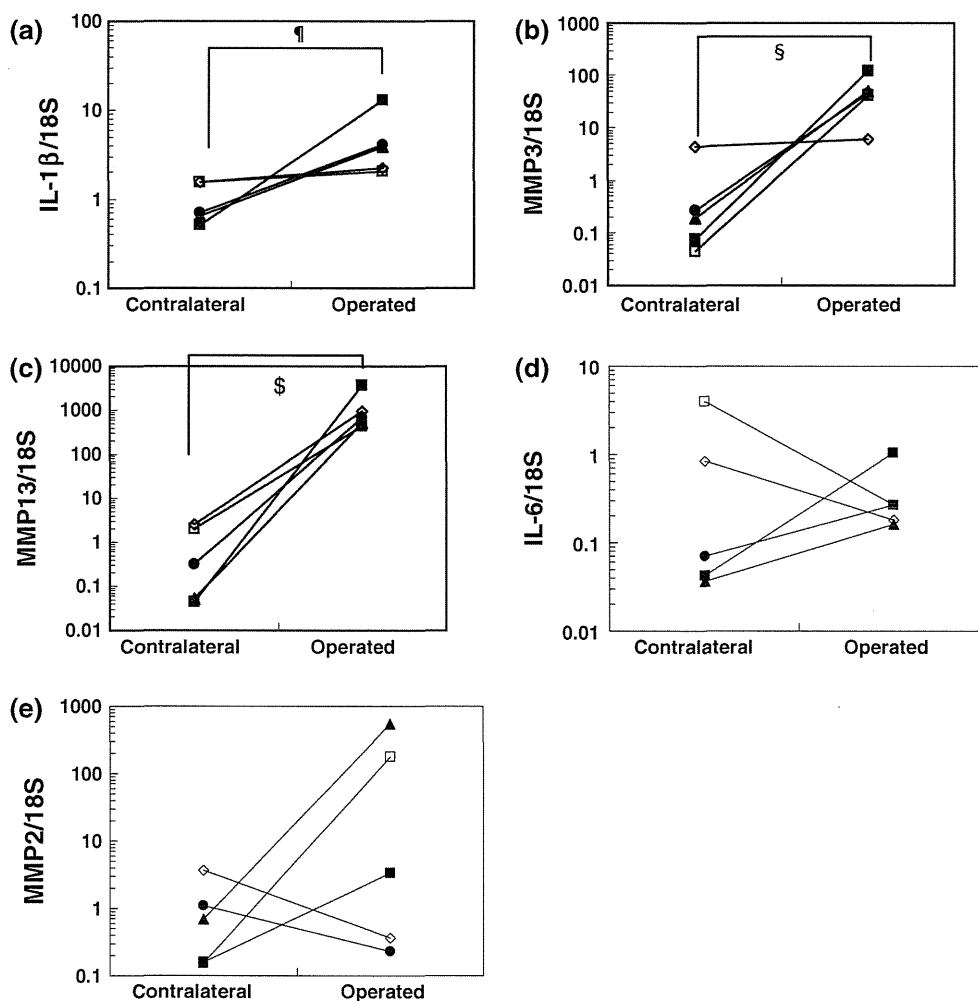


**Fig. 1** mRNA levels for inflammatory mediators and MMPs in the SM after surgery. Quantification of the results of RT-qPCR for inflammatory mediators and MMPs including IL-1 $\beta$  (a), MMP-3 (b), MMP-13 (c), IL-6 (d), and MMP-2 (e) normalized to 18S in SM from the operated and contralateral knees of the sheep at 2 weeks after

surgery. mRNA extraction failed from one sheep under ACL reconstruction surgery. ¶ $p = 0.006$ , § $p = 0.009$ , § $p = 0.006$ . Filled triangle, filled square, filled circle, open diamond, open square: sheep 1–5

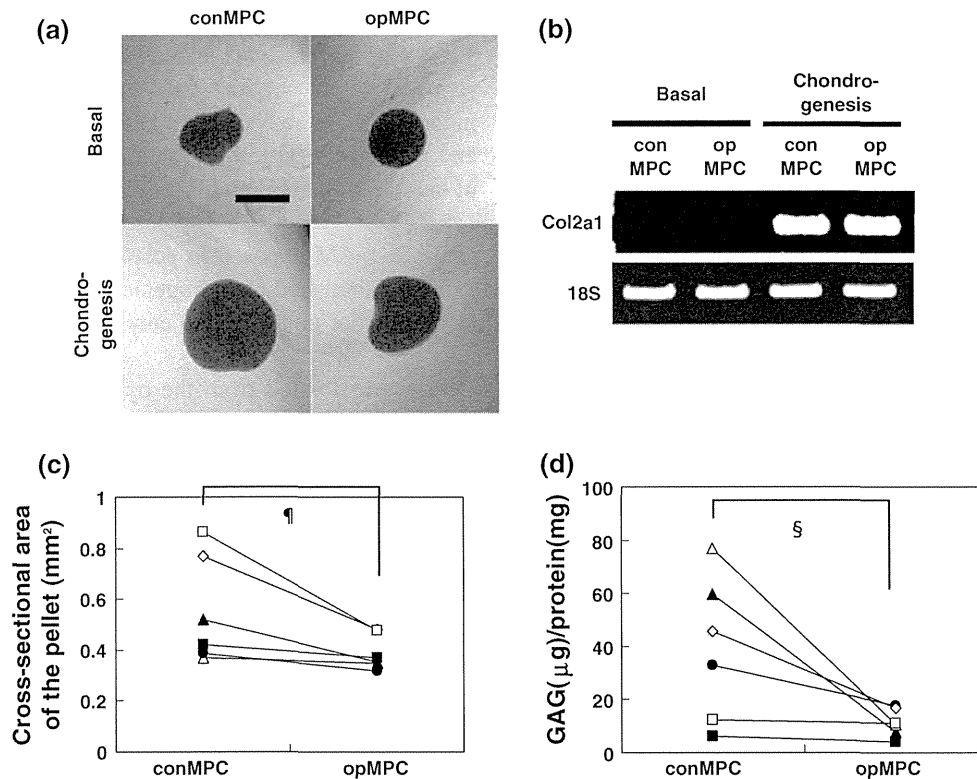


**Fig. 2** Comparison of the chondrogenic potential between opMPC and conMPC. **a** A photograph of cell pellets from opMPC and conMPC cultured in basic culture medium (control) or chondrogenic medium (chondrogenesis). Bar 500 μm. **b** mRNA analysis of conMPC and opMPC for chondrogenic marker gene, type II collagen

(*Col2a1*), and 18S. **c** The cross-sectional area from a representative 2D image of cell pellets. <sup>†</sup> $p = 0.02$ . **d** The measurement of GAG by cell pellets normalized to protein level. <sup>§</sup> $p = 0.004$ . Filled triangle, filled square, filled circle, open diamond, open square, open triangle: sheep 1–6

medium for both opMPC and conMPC (Fig. 2a). RT-PCR analysis confirmed elevated mRNA expression for type II collagen for both cell sources cultured in chondrogenic medium (Fig. 2b). Measurement of the cross-sectional area of the opMPC pellets ( $0.390 \pm 0.0690 \text{ mm}^2$ ) revealed they were significantly smaller than the corresponding conMPC pellets ( $0.554 \pm 0.210 \text{ mm}^2$ ,  $p = 0.02$ ) (Fig. 2c). The glycosaminoglycan content of the conMPC pellets cultured in the chondrogenic medium ( $39.0 \pm 27.4 \text{ GAG/protein}$ ) was significantly higher than those of the opMPC pellets ( $11.4 \pm 5.22 \text{ GAG/protein}$ ,  $p = 0.004$ ) (Fig. 2d). These data suggest that surgery-associated inflammation appeared to have a deleterious influence on the chondrogenic potential of MPCs derived from the SM.

Cells from SM exposed to post-surgery inflammation exhibit osteogenic and adipogenic potential similar to cells from the non-operated contralateral knees

Both opMPCs and conMPCs cultured in osteogenic medium were stained with Alizarin Red; however, cells cultured in basal medium did not stain (Fig. 3a). Calcium deposition by opMPCs cultured in osteogenic medium

( $6.84 \pm 2.56 \text{ μg/ml}$ ) was similar to that of corresponding conMPCs ( $6.47 \pm 2.90 \text{ μg/ml}$ ) (Fig. 3b). Furthermore, the adipogenic potential of both cell populations was also examined. Oil Red O staining showed that cells cultured in control medium did not stain with Oil Red O to any detectable extent, while cells from both knees of the two groups cultured in adipogenic medium did stain in a detectable manner (Fig. 3c). The eluates of associated Oil Red O revealed no significant differences in lipid accumulation between opMPCs ( $0.100 \pm 0.095 \text{ OD}$ ) and conMPCs ( $0.118 \pm 0.102 \text{ OD}$ ) (Fig. 3d).

Cells from SM exposed to post-surgery inflammation continue to over-express mRNA for IL-1 $\beta$  and MMP-3 and -13

Cells isolated from the operated (opMPC) and contralateral (conMPC) knees retained the mesenchymal multi-lineage differentiation potencies, as shown in Figs. 2, 3. These cells were therefore defined as mesenchymal progenitor cells (MPCs). To investigate the effect of an altered intraarticular environment on cells isolated from the tissue exposed to inflammation, mRNA levels for catabolic

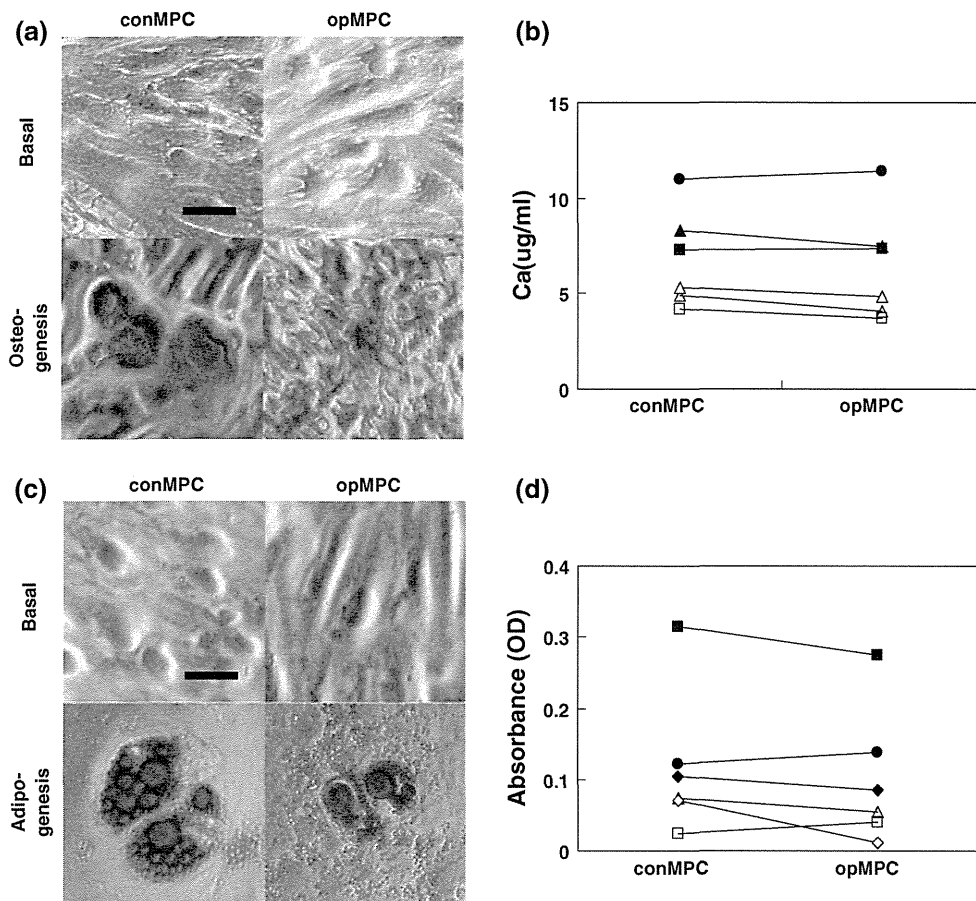


**Fig. 3** Comparison of the osteogenic and adipogenic potential between opMPC and conMPC. **a** Photomicrographs of opMPC and conMPC cultured in basic culture medium (control) or osteogenic medium (osteogenesis) stained with alizarin red. *Bar* 25 μm. **b** Calcium content of cells cultured in osteogenic medium. **c** Photomicrographs of opMPC and conMPC cultured in basic culture

medium (control) or adipogenic induction medium (adipogenesis) stained with oil red O. *Bar* 25 μm. **d** Elution of Oil Red O from opMPC and conMPC following exposure to adipogenic medium. *Filled triangle, filled square, filled circle, open diamond, open square, open triangle*: sheep 1–6. No significant differences were detected

biomarkers between opMPCs and conMPCs at passage 2 were compared. Quantitative RT-PCR revealed that mRNA levels for IL-1β, MMP-3, and MMP-13 normalized to 18S in opMPCs remained somewhat higher than those in conMPCs; however, significant differences were not detected due to large animal-to-animal variation (Fig. 4a–c). Trends for higher mRNA levels for MMP-13 (Fig. 4c) in opMPCs compared to the corresponding conMPCs were observed in all animals, while such trends were observed for IL-1β (Fig. 4a) and MMP-3 (Fig. 4b) in cells from five of six animals.

**Effect of exogenous IL-1β on the chondrogenic potential of SM-derived normal cells**

To examine the potential involvement of inflammatory mediators in the observed inhibition of chondrogenesis by cells from surgically affected joints, 0–100 nM of IL-1β

were added during the chondrogenic differentiation of MPCs from normal sheep SM. The cross-sectional area of normal SM-MPC pellets cultured in the chondrogenic medium with >1 nM IL-1β were significantly reduced compared to those cultured in chondrogenic medium without IL-1β (Fig. 5).

**Discussion**

In this study, it has been demonstrated that surgical intervention to the ovine knee joint results in increases in the volume of SF in the joints, as well as elevations in mRNA levels for some catabolic biomarkers in the corresponding SM by 2 weeks post-surgery. In addition, and critical to the effectiveness of endogenous MPCs, it was demonstrated that cells from SM exposed to surgery-associated inflammation maintained over-expression of inflammatory

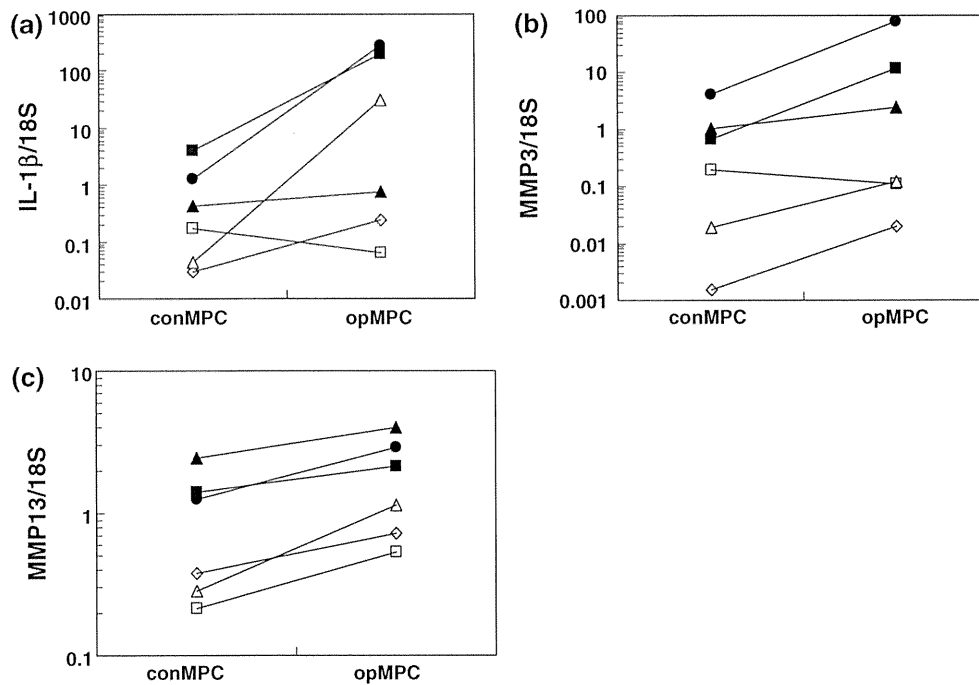


**Fig. 4** mRNA levels for inflammatory mediators and MMPs in the SM after surgery. Quantification of the results of RT-qPCR analysis inflammatory mediators and MMPs including IL-1 $\beta$  (a), MMP-3 (b), and MMP-13 (c) normalized to 18S in SM-MPCs derived from the

operated (*opMPC*) and contralateral (*conMPC*) knees of the sheep at 2 weeks after ACL reconstruction surgery. Filled triangle, filled square, filled circle, open diamond, open square, open triangle: sheep 1–6

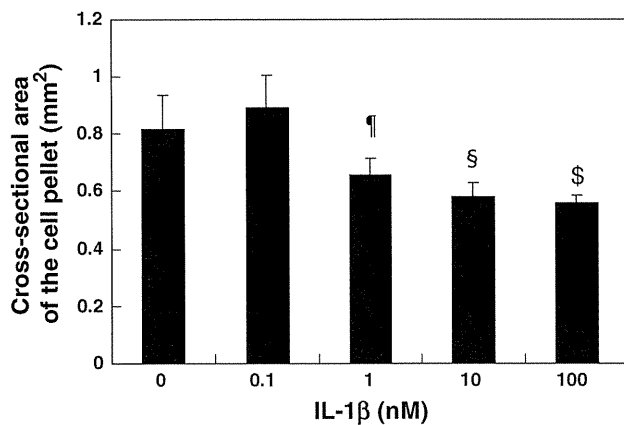


**Fig. 5** Chondrogenic potential under IL-1 $\beta$  stimulation: ratio of sectional area from 2D images of MPCs from normal sheep SM cultured in chondrogenic induction medium with 0–100 nM IL-1 $\beta$ . <sup>¶</sup> $p = 0.01$ , <sup>§</sup> $p < 0.001$ , <sup>§</sup> $p < 0.001$  compared to MPC pellets cultured in chondrogenic induction medium without IL-1 $\beta$ .  $N = 4$

biomarkers and uniquely exhibited lower chondrogenic differentiation capacity ( $\sim 70\%$  of control values) compared to cells from the contralateral knee. It was also shown that in-vitro exposure to 1–100 nM of exogenous IL-1 $\beta$  also led to diminished chondrogenic differentiation capacity of SM-MPCs from normal sheep.

Inflammatory mediators including IL-1 $\beta$  and TNF $\alpha$  have been reported to decrease the mRNA levels for

chondrogenic markers including Col2A1 and aggrecan during chondrogenesis of BM-MSCs and SM-MSCs, respectively, under the influences of BMP2 in a dose-dependent manner [35, 36]. These inflammatory mediators were also reported to inhibit chondrogenesis induced by TGF $\alpha$  [37], as well as osteogenesis [38] by human BM-MSCs. The present results and the reports from other laboratories suggest that inflammatory cytokines are potentially involved in the suppression of the chondrogenic capacity of cells exposed to inflammation, and that this suppressive effect on chondrogenic capacity by MPCs exposed to inflammation may also contribute to the unstable balance between degradative and biosynthetic events within the joints, an imbalance which could ultimately contribute to OA development and progression.

In contrast to other reports with human BM-MSCs [38], we did not detect differences in osteogenic and adipogenic potential between cells isolated from the SM from operated knees compared to those from contralateral knees. We speculate that part of this discrepancy may be based on the relatively low osteogenic/adipogenic potential of the cells derived from the SM compared to their chondrogenic potential, or perhaps species or tissue origin differences.

Metalloproteinases are reported to play central roles in tissue repair and remodeling of connective tissues in response to injury, as well as being involved in destructive disease processes including OA [39]. They are sub-grouped

into collagenases (MMP-1, MMP-8, MMP-13, and MMP-18), gelatinases (MMP-2 and MMP-9), stromelysins (MMP-3, MMP-10, and MMP-11), matrilysins, membrane-type (MT)-MMPs, and others [40]. In the present study, mRNA levels for MMP-3 and MMP-13 in SM tissue from operated knees were significantly higher than those from contralateral knees, but the differences in mRNA levels for MMP-2 were trends only. MMPs are synthesized as pre-proenzymes and processed by tissue and plasma proteinase including other active MMPs to become active MMPs that can digest a number of ECM molecules including collagens and aggrecans [40]. Furthermore, several of the differences in mRNA levels for MMPs between conMPC and opMPC were also only trends; however, GAG measurement in chondrogenic cell pellets showed significant differences between conMPC and opMPC cultures.

With regard to the effect of exogenous IL-1 $\beta$  on chondrogenic differentiation of normal SM-MPCs, a number of interesting points are raised by the data. First, exposure to IL-1 $\beta$  led to decreases in chondrogenesis to  $\sim 70\%$  of control values. This level of decline was similar to that detected between the opMPC and conMPC cultures. However, it remains to be determined whether IL-1 $\beta$  is the primary endogenous effector cytokine *in vivo*. Secondly, the inhibition of chondrogenesis following exposure to the exogenous IL-1 $\beta$  appeared to be nearly maximal with 10 nM of IL-1 $\beta$  and no further declines were detected when concentrations were increased to 100 nM. Thus, it would appear that only a subset of SM-MPCs are susceptible to the inhibitory influences of this cytokine *in vivo*, and it is curious that there is such correlation between the levels of inhibition of chondrogenesis in the opMPC compared to the conMPC, and the *in-vitro* IL-1 $\beta$  studies. At a minimum, the findings imply there are multiple subsets of MSCs/MPCs in the SM from normal sheep, some being responsive to IL-1 $\beta$  and others resistant to the biological effects of the cytokine. Whether such response patterns relate to expression of IL-1 receptors by a subset of MPCs is the subject of current studies.

While the results presented clearly show how inflammation in the surgically altered knee joint leads to decreased potential for synovial membrane MSCs to differentiate towards the chondrogenic phenotype, there are some limitations to the studies presented. First, the number of animals assessed is not large. However, we have used a large animal model and it is difficult to use a substantial number due to cost and ability to house and train large numbers of animals. This limitation is off-set by using a large animal with knee components not unlike those of the human. Second, we are able to obtain as much synovial fluid as possible, but have no way of determining whether we obtained all of it when trying to quantify volumes. However, the method used was reproducible in our hands. Thirdly, we obtained synovial

membranes from reproducible sites, but we do not know if there are site-specific differences, and whether the altered proteinase levels contributed to the selective release of subsets of MSCs from the synovium which could have influenced the findings. Fourthly, we measured mRNA, but not corresponding protein levels so cannot with certainty say the mRNA levels led to alterations in protein levels for specific molecules. Moreover, an additional limitation of this study is that only one point of the acute post-surgery stage was investigated. It has been reported that IL-6 and TNF $\alpha$  levels in SF decline with time after ACL injury, but remain considerably elevated chronically (3 months) [13]. It remains unclear whether the prolonged exposure of the MPCs to chronic inflammation would further compromise mRNA levels for relevant molecules and chondrogenic capacities. Further investigation will be needed to clarify the potential influence of duration of exposure to inflammation on the function of the cells and whether they recover function *in vitro* with increasing cell passage number. Such issues are the subject of current studies. Finally, we only assessed mRNA levels for a few molecules, and future studies should expand the repertoire of molecules assessed. In spite of these limitations, the results presented are novel and indicate that the joint environment can influence the phenotype of the synovial membrane-associated MSCs.

We conclude that cells from tissue exposed to post-surgery inflammation continue to over-express inflammatory biomarkers that can affect the chondrogenic potential of MPCs, suggesting that MPCs from injured joints are compromised and retain the compromised phenotype regarding their endogenous repair potential.

**Acknowledgments** We thank Craig Sutherland and Carol Reno for technical assistance with the sheep surgery and the RT-qPCR analysis, respectively. The authors also thank Dr. Yamini Achari for editorial assistance. This research was supported by the Uehara Memorial Foundation, an Osteoarthritis Team Grant from the Alberta Heritage Foundation for Medical Research, a CHIR grant to C.B.F. and N.G.S. focussed on the sheep model, and the CIHR Institute for the Gender and Health. D.A.H. is the Calgary Foundation–Grace Glaum Professor and C.B.F. is the McCaig Professor. W.A. is a fellow of the UMF and AHFMR.

**Conflict of interest** The authors report no conflict of interest. The authors alone are responsible for the content and writing of the paper.

## References

1. Pittenger MF, Mackay AM, Beck SC, Jaiswal RK, Douglas R, Mosca JD, et al. Multi-lineage potential of adult human mesenchymal stem cells. *Science*. 1999;284:143–7.
2. Jankowski RJ, Deasy BM, Huard J. Muscle-derived stem cells. *Gene Ther*. 2002;9:642–7.
3. De Bari C, Dell’Accio F, Tylzanowski P, Luyten FP. Multipotent mesenchymal stem cells from adult human synovial membrane. *Arthritis Rheum*. 2001;44:1928–42.



4. Wickham MQ, Erickson GR, Gimble JM, Vail TP, Guilak F. Multipotent stromal cells derived from the infrapatellar fat pad of the knee. *Clin Orthop*. 2003;412:196–212.
5. Lee OK, Kuo TK, Chen WM, Lee KD, Hsieh SL, Chen TH. Isolation of multipotent mesenchymal stem cells from umbilical cord blood. *Blood*. 2003;103:1669–75.
6. Miao Z, Jin J, Chen L, Zhu J, Huang W, Zhao J, et al. Isolation of mesenchymal stem cells from human placenta: comparison with human bone marrow mesenchymal stem cells. *Cell Biol Int*. 2006;30:681–7.
7. Sakaguchi Y, Sekiya I, Yagishita K, Muneta T. Comparison of human stem cells derived from various mesenchymal tissues: superiority of synovium as a cell source. *Arthritis Rheum*. 2005;52:2521–9.
8. Ando W, Tateishi K, Hart DA, Katakai D, Tanaka Y, Nakata K, et al. Cartilage repair using in vitro generated scaffold-free tissue engineered construct derived from porcine synovial mesenchymal stem cells. *Biomaterials*. 2007;28:5462–70.
9. Mor A, Abramson SB, Pillinger MH. The fibroblast-like synovial cell in rheumatoid arthritis: a key player in inflammation and joint destruction. *Clin Immunol*. 2005;115(2):118–28.
10. Jones EA, English A, Henshaw K, Kinsey SE, Markham AF. Enumeration and phenotypic characterization of synovial fluid multipotential mesenchymal progenitor cells in inflammatory and degenerative arthritis. *Arthritis Rheum*. 2004;50:817–27.
11. Harvanová D, Tóthová T, Sarišský M, Amrichová J, Rosocha J. Isolation and characterization of synovial mesenchymal stem cells. *Folia Biol (Praha)*. 2011;57(3):119–24.
12. Fernandes JC, Martel-Pelletier J, Pelletier JP. The role of cytokines in osteoarthritis pathophysiology. *Biorheology*. 2002;39:237–46.
13. Cameron M, Buchgraber A, Passler H, Vogt M, Thonar E, Fu F, et al. The natural history of the anterior cruciate ligament-deficient knee. Changes in synovial fluid cytokine and keratan sulfate concentrations. *Am J Sports Med*. 1997;25:751–4.
14. Irie K, Uchiyama E, Iwaso H. Intraarticular inflammatory cytokines in acute anterior cruciate ligament injured knee. *Knee*. 2003;10:93–6.
15. Higuchi H, Shirakura K, Kimura M, Terauchi M, Shinozaki T, Watanabe H, et al. Changes in biochemical parameters after anterior cruciate ligament injury. *Int Orthop*. 2006;30:43–7.
16. Marks PH, Donaldson ML. Inflammatory cytokine profiles associated with chondral damage in the anterior cruciate ligament-deficient knee. *Arthroscopy*. 2005;21:1342–7.
17. Tung JT, Fenton JJ, Arnold C, Alexander L, Yuzbasiyan-Gurkan V, Venta PJ, et al. Recombinant equine interleukin-1beta induces putative mediators of articular cartilage degradation in equine chondrocytes. *Can J Vet Res*. 2002;66:19–25.
18. Jasser MZ, Mitchell PG, Cheung HS. Induction of stromelysin-1 and collagenase synthesis in fibrochondrocytes by tumor necrosis factor-alpha. *Matrix Biol*. 1994;14:241–9.
19. Murphy JM, Dixon K, Beck S, Fabian D, Feldman A, Barry F. Reduced chondrogenic and adipogenic activity of mesenchymal stem cells from patients with advanced osteoarthritis. *Arthritis Rheum*. 2002;46:704–13.
20. Alsalameh S, Amin R, Gemba T, Lotz M. Identification of mesenchymal progenitor cells in normal and osteoarthritic human articular cartilage. *Arthritis Rheum*. 2004;50:1522–32.
21. Dudics V, Kunštár A, Kovács J, Lakatos T, Géher P, Gömör B, et al. Chondrogenic potential of mesenchymal stem cells from patients with rheumatoid arthritis and osteoarthritis: measurements in a microculture system. *Cells Tissues Organs*. 2009;89:307–16.
22. Scharstuhl A, Mutsaers HA, Pennings SW, Szarek WA, Russel FG, Wagener FA. Chondrogenic potential of human adult mesenchymal stem cells is independent of age or osteoarthritis etiology. *Stem Cells*. 2007;25:3244–51.
23. Frank CB, Jackson DW. The science of reconstruction of the anterior cruciate ligament. *J Bone Joint Surg Am*. 1997;79:1556–76.
24. Fleming BC, Hulstyn MJ, Oksendahl HL, Fadale PD. Ligament injury reconstruction and osteoarthritis. *Curr Opin Orthop*. 2005;16:354–62.
25. Heard BJ, Achari Y, Chung M, Shrive NG, Frank CB. Early joint tissue changes are highly correlated with a set of inflammatory and degradative synovial biomarkers after ACL autograft and its sham surgery in an ovine model. *J Orthop Res*. 2011;29(8):1185–92.
26. Kuh SU, Zhu Y, Li J, Tsai KJ, Fei Q, Hutton WC, et al. Can TGF-beta1 and rhBMP-2 act in synergy to transform bone marrow stem cells to discogenic-type cells? *Acta Neurochir (Wien)*. 2008;150:1073–9.
27. Tateishi K, Higuchi C, Ando W, Nakata K, Hashimoto J, Hart DA, et al. The immunosuppressant FK506 promotes development of the chondrogenic phenotype in human synovial stromal cells via modulation of the Smad signaling pathway. *Osteoarthr Cartil*. 2007;15:709–18.
28. Magari K, Nishigaki F, Sasakawa T, Ogawa T, Miyata S, Ohkubo Y, et al. Anti-arthritis properties of FK506 on collagen-induced arthritis in rats. *Inflamm Res*. 2003;52:524–9.
29. Reno C, Marchuk L, Sciore P, Frank CB, Hart DA. Rapid isolation of total RNA from small samples of hypocellular, dense connective tissues. *Biotechniques*. 1997;22:1082–6.
30. Nakajima I, Muroya S, Chikuni K. Growth arrest by octanoate is required for porcine preadipocyte differentiation. *Biochem Biophys Res Commun*. 2003;309:702–8.
31. Hong L, Colpan A, Peptan IA. Modulations of 17-beta estradiol on osteogenic and adipogenic differentiations of human mesenchymal stem cells. *Tissue Eng*. 2006;12:2747–53.
32. Hellio Le Graverand MP, Reno C, Hart DA. Heterogenous response of knee cartilage to pregnancy in the rabbit: assessment of specific mRNA levels. *Osteoarthr Cartil*. 2000;8:53–62.
33. Lu T, Achari Y, Rattner JB, Hart DA. Evidence that estrogen receptor beta enhances MMP-13 promoter activity in HIG-82 cells and that this enhancement can be influenced by ligands and involves specific promoter sites. *Biochem Cell Biol*. 2007;85:326–36.
34. Zou L, Zou X, Chen L, Li H, Mygind T, Kassem M, et al. Multilineage differentiation of porcine bone marrow stromal cells associated with specific gene expression pattern. *J Orthop Res*. 2008;26:56–64.
35. Majumdar MK, Wang E, Morris EA. BMP-2 and BMP-9 promotes chondrogenic differentiation of human multipotential mesenchymal cells and overcomes the inhibitory effect of IL-1. *J Cell Physiol*. 2001;189:275–84.
36. Okuma-Yoshioka C, Seto H, Kadono Y, Hikita A, Oshima Y, Kurosawa H, et al. Tumor necrosis factor-alpha inhibits chondrogenic differentiation of synovial fibroblasts through p38 mitogen activating protein kinase pathways. *Mod Rheumatol*. 2008;18:366–78.
37. Wehling N, Palmer GD, Pilapil C, Liu F, Wells JW, Müller PE, et al. Interleukin-1beta and tumor necrosis factor alpha inhibit chondrogenesis by human mesenchymal stem cells through NF-kappaB-dependent pathways. *Arthritis Rheum*. 2009;60:801–12.
38. Lacey DC, Simmons PJ, Graves SE, Hamilton JA. Proinflammatory cytokines inhibit osteogenic differentiation from stem cells: implications for bone repair during inflammation. *Osteoarthr Cartil*. 2009;17:735–42.
39. Murphy G, Nagase H. Reappraising metalloproteinases in rheumatoid arthritis and osteoarthritis: destruction or repair? *Nat Clin Pract Rheumatol*. 2008;4:128–35.
40. Nagase H, Visse R, Murphy G. Structure and function of matrix metalloproteinases and TIMPs. *Cardiovasc Res*. 2006;69:562–73.

# Morphological Observations of Mesenchymal Stem Cell Adhesion to a Nano-Periodic Structured Titanium Surface Patterned Using Femtosecond Laser Processing

Kei Oya<sup>1</sup>, Shun Aoki<sup>2</sup>, Kazunori Shimomura<sup>3</sup>, Norihiko Sugita<sup>3</sup>, Kenji Suzuki<sup>4</sup>,  
Norimasa Nakamura<sup>3</sup>, and Hiromichi Fujie<sup>2,1\*</sup>

<sup>1</sup> *Research Institute for Science and Technology, Kogakuin University, 2665-1 Nakano-machi, Hachioji-city, Tokyo 192-0015, Japan*

<sup>2</sup> *Graduate School of System Design, Tokyo Metropolitan University, 6-6 Asahigaoka, Hino-city, Tokyo 191-0065, Japan*

<sup>3</sup> *Graduate School of Medicine, Osaka University, 2-2 Yamadaoka, Suita-city, Osaka 565-0871, Japan*

<sup>4</sup> *Department of Mechanical Systems Engineering, Kogakuin University, 2665-1 Nakano-machi, Hachioji-city, Tokyo 192-0015, Japan*

## **Abstract:**

It is known that the adhesive and anisotropic properties of cell-derived biomaterials are affected by micro- or nano-scale structures processed on culture surface. In the present study, the femtosecond laser processing technique was used to scan a laser beam at an intensity around ablation threshold level on a titanium surface for nano-scale processing. Microscopic observation revealed that the processed titanium exhibited a periodic-patterned groove structure at the surface; the width and depth of the groove were  $292 \pm 50$  nm and  $99 \pm$

31 nm, respectively, and the periodic pitch of the groove was  $501 \pm 100$  nm. Human synovium-derived mesenchymal stem cells were cultured on the surface at the cell density of  $3.0 \times 10^3$  cells/cm<sup>2</sup> after 4-time cell passage. For comparison, the cells were also cultured on a non-processed titanium surface at the condition identical to the processed surface. Results revealed that the duration for cell attachment to the surface was dramatically reduced on the processed titanium as compared with the non-processed titanium. Moreover, on the processed titanium, cell extension area was significantly increased while cell orientation was aligned along the direction of the periodic grooves. These results suggest that the femtosecond laser processing improves the adhesive and anisotropic properties of cells by producing the periodic nano-scale structure on titanium culture surfaces.

\* Corresponding author. Phone/fax: +81 42 585 8628

E-mail address: [fujie@sd.tmu.ac.jp](mailto:fujie@sd.tmu.ac.jp)

## 1. Introduction

Titanium and its alloys are widely used as implant biomaterials because they have various excellent properties as follows: [1] high-specific strength and good corrosion resistance, [2] mechanically compatible Young's modulus lower than those of stainless steels and cobalt-chromium alloys, and [3] no cytotoxicity to a living body. Various biofunctions such as adhesiveness and anisotropy are required for biomaterials and medical devices depending on body parts to which they are applied. The most simple and effective method for providing metals with those biofunctions may be the use of surface treatment and modification techniques. Numerous research groups have improved the biocompatibility of biomaterials using the techniques and some of them have already been commercialized.

A biofunction required for most of biomaterials is adequate cell adhesiveness. It has been demonstrated that a material surface processed in micro- or nano-level promotes the cellular adhesiveness.<sup>1-3)</sup> Widely spread and the most convenient method of materials is etching process; chemical etching<sup>4,5)</sup> or electrochemical etching<sup>6,7)</sup> so called wet etching, and ion beam processing<sup>8,9)</sup> or reactive ion etching<sup>10,11)</sup> so called dry etching. A lot of substrates can be created at a short time with low-cost in wet etching, while a processing with high aspect ratio is possible with a variety of choices for patterns and material in dry etching. However, in wet and dry etching, it was problematic that chemical components remained on the material surfaces are harmful to cells and cell-derived biomaterials. On the other hand, laser processing is a clean technique for surface processing and modification through physical phenomena such as melting or evaporating. Therefore, it is free from chemical contamination on a laser-processed surface. Laser beam processing is categorized into thermal processing and ablation processing. Although the former can be applied to many objects, processed surface may be oxidized by heating. As a result, the composition and

thickness of surface oxide layer are changed in case of metal. The latter, laser ablation, can solve the above-described problem and can be usually performed by the use of femtosecond laser processing system. The laser system can irradiate a fine ranged laser beam with a strong intensity because the laser pulse is compressed to a femtosecond level. Therefore, the heat damages are mostly suppressed, since the laser irradiation breaks up before energy transfer from electrons to lattice ions and the heat-affected zone is quite small.<sup>12)</sup> Previous studies reported that a nano-sized grating (periodic structures) or dots were formed on material surfaces using femtosecond laser processing.<sup>13,14)</sup> Therefore, it is expected that the femtosecond laser processing is useful for surface modification of biomaterials.

Stem cell-based therapies have great potentials for the repair and regeneration of tissues or organs lost or damaged with any reasons such as accidents or diseases. Some of the co-authors of the present study have developed a novel tissue-engineering technique for tissue repair using a stem cell-based self-assembled tissue (scSAT) bio-synthesized from synovium-derived mesenchymal stem cells.<sup>15)</sup> The scSAT consists of abundant type I and type III collagens, fibronectin and vitronectin, which are thought to be important constituents for tissue repair. Moreover, the scSAT is a scaffold-free construct composed of synovium-derived mesenchymal stem cells with their native extracellular matrices, it is free from concern regarding long-term immunological effects. Therefore, the scSAT is expected as a novel material for regenerative medicine, in particular for the repair of ligaments and tendons. However, the mechanical properties of the scSAT were insufficient for clinical application. Moreover, the structural and mechanical properties of the scSAT are isotropic while those of ligaments and tendons are anisotropic. To the problem, it may be a candidate of solutions to promote the generation of extracellular matrix in the scSAT by means of a special culture on a nano-structured surface. As described above, previous studies indicated that a material having a certain roughness promotes cell adhesiveness and that a material

having a periodic-pattern increases anisotropic property of cells.<sup>10)</sup>

Therefore, a nano-periodic patterned structure was processed on a titanium surface using a femtosecond laser system, and the adhesive and anisotropic properties of human synovium-derived mesenchymal stem cells to the processed surface were determined in the present study.

## **2. Materials and methods**

### **2.1 Preparation of titanium specimens**

Commercially available pure titanium disks with grade 2 (19 mm $\phi$  x 1.5 mm in thickness; Rare Metallic Co., Ltd., Tokyo, Japan) were wet-polished with SiC papers of grit number of 320, 600, 800, and 1,000 in the increasing order (Refinotec Co., Ltd., Kanagawa, Japan). Then, they were ultrasonically rinsed in acetone for 10 min and dried with air using an air pump. They were kept in an auto-dry desiccator. These titanium disks are named “Ti”.

The nano-periodic structure on a Ti surface was patterned using a femtosecond laser apparatus (IFRIT, Cyber Laser Inc., Japan) with a seed laser (Femtolute, IMRA America Inc., Ann Arbor, MI, USA). The processing conditions were as follows: irradiation intensity of 700 mW, pulse repetition frequency of 1 kHz, pulse width of 190 fs, wavelength of 780 nm, beam diameter of 6 mm, focal distance of 60 mm, and scanning speed of 10 mm/s. The laser irradiation was defocused for 7 mm from the focal point. The titanium specimens subjected to nano-periodic processing are named “Nano-Ti”.

### **2.2 Surface observation and characterization**